Progress In Electromagnetics Research Letters, Vol. 99, 153–157, 2021

Topological Optimization Method for Ship Detection in SAR Images

Dianqi Pei and Meng Yang*

Abstract—The aim of this study is to provide a topological optimization method for ship detection in synthetic aperture radar (SAR) imagery. The method consists of three steps: pre-processing, sparse representation, and classification. For the first step, the variational model is used for SAR image filtering. For the second step, the curvature of the surface manifold is constructed for sparse representation of target. For the third step, the topological derivative method is adopted to locate the target. Experiments show that the proposed method is effective in reducing false alarms, and obtains a satisfactory detection performance.

1. INTRODUCTION

With its all-weather and all-time capabilities, synthetic aperture radar (SAR) remote sensing has great potential for real-time ocean observations [1]. Due to the different backscattering characteristics of different ocean objects, SAR images can provide discriminant features for the understanding and interpretation of reliable scenes [2]. In the past decades, the amount of SAR image data increases with increasing resolution, which has been used for fishery monitoring, warship reconnaissance, marine waste monitoring, oil spill detection, migration control, and many other tasks [3]. As an important application, ship detection in SAR image has been widely studied, and many classical detection methods have been designed in the framework of automatic target recognition (ATR) of SAR [4].

The key ideas in ship detection is how to take advantage of the distinguishable characteristics between ship targets and surrounding sea clutter [5]. Under most circumstances, pixel values of targets in SAR image are unusually bright compared to those in the surrounding area [6]. Thus, ship detection can be achieved by searching for pixels whose intensity levels are greater than an adaptive threshold. Among these, the constant false alarm rate (CFAR) based on statistic models is the most commonly used and most popular method of ship detection in SAR images [7]. Based on the hypothesis test, the method looks for the adaptive threshold according to the background distribution to keep the false alarm rate at the predetermined level. The performance of CFAR detection depends on the design of sliding window, statistical modeling of clutter distribution, and estimation of model parameters [8]. Subsequent works mainly focus on these aspects to design effective detection algorithms [9]. Over the years, many window structures and statistical models have been designed in the CFAR framework to deal with clutter and complex background distributions [10]. However, with the increasing complexity of the model, parameter estimation becomes a difficult problem and even limits the real application of CFAR technology. Because of the non-homogeneous and non-stationary characteristics of the sea clutter in SAR images, these methods are insensitive to different scale ships, especially for small scale ships.

In this article, we propose a new ship detection scheme, which considers both topological structure and sparsity of matrix, can effectively eliminate false alarm, and achieves a good performance for ship detection in SAR image.

Received 29 April 2021, Accepted 6 August 2021, Scheduled 21 August 2021
* Corresponding author: Meng Yang (yangmeng@hdu.edu.cn).
The authors are with the College of Communication Engineering, Hangzhou Dianzi University, Hangzhou, China.

2. PROPOSED METHODS

For the first step, a preprocessing technique is presented, which is based on the framework of variational approach and energy functional minimization. Without loss of generality, we restrict ourselves to the following energy functional

$$\mathcal{L}(I_f) = 2^{-1} \int_\Omega (I_f - I_o)^2 d\Omega + \lambda \int_\Omega \mathcal{F}\left(\|\nabla I_f\|\right) d\Omega \tag{1}$$

where I_o denotes the SAR image data, I_f the filtered image data, ∇ the gradient operator, λ the weight parameter, Ω the local neighborhood, and $\|\ \|$ the vector norm. The following Euler equation for this energy functional is obtained.

$$I_o = I_f - \lambda \mathrm{div}\left\{\mathcal{F}'\left(\|\nabla I_f\|\right)\left(\|\nabla I_f\|\right)^{-1}\nabla I_f\right\} \tag{2}$$

and

$$\mathcal{F}' = \|\nabla I_f\| \left(\|G_\sigma * \nabla I_f\|^2 + \eta^2\right)^{-\frac{\rho}{2}} \tag{3}$$

where $\mathcal{F}'$ denotes the derivative of $\mathcal{F}$, $\rho \in (1,2)$; G_σ is a Gaussian filter; σ denotes the standard deviation; $*$ denotes the convolution operator; and $\eta > 0$ is the conductance parameter.

For the second step, an approach is presented to estimate mean curvature $\mathcal{H}$ on point-sampled surface I_f according to the principle of differential geometry.

$$\mathcal{H}\left(I_f\right) = \frac{1}{2}\left[1 + \left(\frac{\partial I_f}{\partial x}\right)^2 + \left(\frac{\partial I_f}{\partial y}\right)^2\right]^{-\frac{3}{2}} \mathcal{K}\left(I_f\right) \tag{4}$$

and

$$\mathcal{K}\left(I_f\right) = \Delta I_f + \left(\frac{\partial I_f}{\partial y}\right)^2 \frac{\partial^2 I_f}{\partial x^2} + \left(\frac{\partial I_f}{\partial x}\right)^2 \frac{\partial^2 I_f}{\partial y^2} - 2\frac{\partial I_f}{\partial x}\frac{\partial I_f}{\partial y}\frac{\partial^2 I_f}{\partial x \partial y} \tag{5}$$

where Δ denotes the Laplacian operator, and the coordinate pair (x, y) indicates pixel position on the image.

For the third step, a energy functional $\mathcal{L}(\psi)$ is constructed [11].

$$\mathcal{L}(\psi) = 2^{-1} \int_\Omega \left[\psi - \left(\mathcal{H}\left(I_f\right) - I_c\right)\right]^2 d\Omega + \kappa \int_\Omega \nabla\psi \nabla\psi d\Omega \tag{6}$$

and ψ is the solution of the equation

$$\int_\Omega \nabla\psi\nabla\varphi d\Omega + \int_\Omega \left[\psi - \kappa\left(\mathcal{H}\left(I_f\right) - I_c\right)\right]\varphi d\Omega = 0 \tag{7}$$

where $\kappa \in (0,1)$, φ denotes any locally-integrable function in the region Ω, and I_c denotes the detection result (a binary images). Using the method proposed in [11], the topological derivative $\mathcal{D}(x,y)$ for each pixel position (x,y) in image $\mathcal{H}(I_f)$ is computed.

$$\mathcal{D}(x,y) = 2^{-1}\left(c_i - I_c\right)\left[\left(\psi\left(x,y\right) - \left(\mathcal{H}\left(I_f\right) - I_c\right)\right) + \left(\psi\left(x,y\right) - \left(\mathcal{H}\left(I_f\right) - c_i\right)\right) + 2\left(1-\kappa\right)\psi\left(x,y\right)\right] \tag{8}$$

where $c_i \in \{0,1\}$ is the intensity associated with the ith class.

We return now to a more detailed algorithm implementation in the above-mentioned theory and methods.

The main steps of the ship detection algorithm are as follows:

Step 1) Variational approach and energy functional minimization are used for filtering SAR image I_o. The filtered image is denoted by I_f.

Step 2) According to the theory of differential geometry, the mean curvature $\mathcal{H}(I_f)$ of I_f is obtained by direct calculation.

Step 3) The targets are segmented from the image $\mathcal{H}(I_f)$ based on the topological derivative $\mathcal{D}$.

3. EXPERIMENTAL RESULTS AND ANALYSIS

We demonstrate the detector performance with real SAR image data. Experiments are carried out in the MATLAB R2017b simulation platform on a Windows-based 64-bit core i3 machine with a 4-GB random access memory. The SAR image is shown in Fig. 1(a). Fig. 1(b) shows the detection result obtained by using the proposed method. The calculation suggests that a period about 35 seconds would have been required.

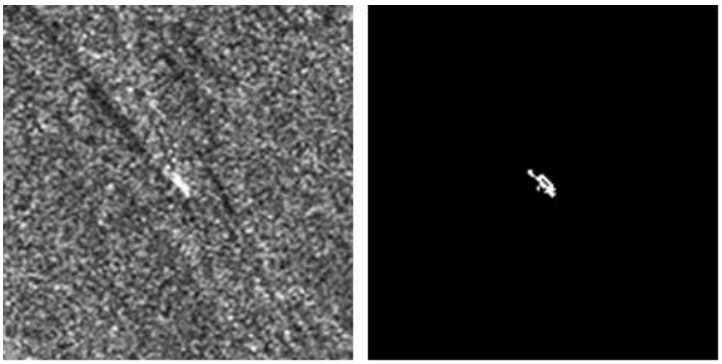

(a) (b)

Figure 1. SAR image I_o and its detected result I_c. (a) Original image. (b) Detected result.

Figure 2 displays SAR image with 3D scene. As shown in Fig. 2, the amplitude of sea clutter data is very complex.

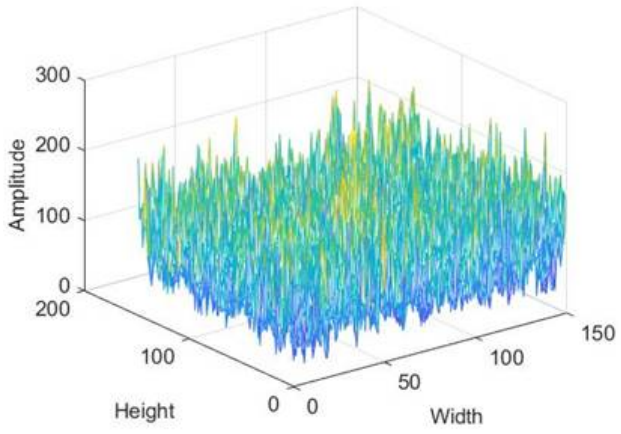

Figure 2. SAR image with 3D scene.

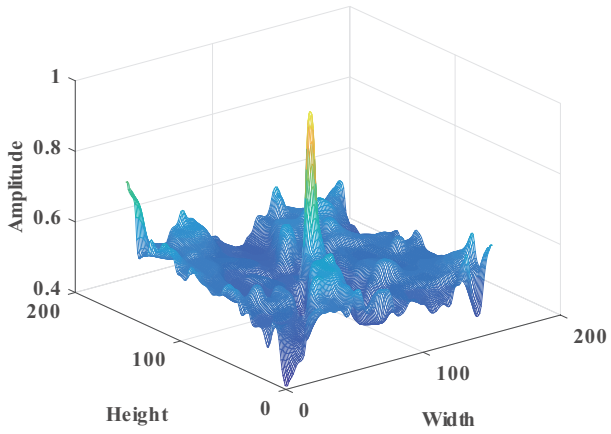

Figure 3. Filtered image I_f with 3D scene.

During the experiments, the first step is to filter SAR image by using variational approach and energy functional minimization against sea clutter. Set the following parameters: the step size $\tau = 5$, $\eta = 10^{-13}$, $\rho = 0.7$, $\sigma = 1$, and the number of iterations $N = 30$. Fig. 3 displays the filtered image I_f with 3D scene.

The second step is to represent target by using mean curvature, which permits a quantitative assessment of the degree of surface smoothing. Fig. 4 displays sparse representation $\mathcal{H}(I_f)$ of filtered image I_f with 3D scene.

The third step is to segment $\mathcal{H}(I_f)$ according to topological derivative information. During the experiments, the parameter value $\kappa = 0.3$. Fig. 5 displays the segmented result I_c of $\mathcal{H}(I_f)$ with 3D scene.

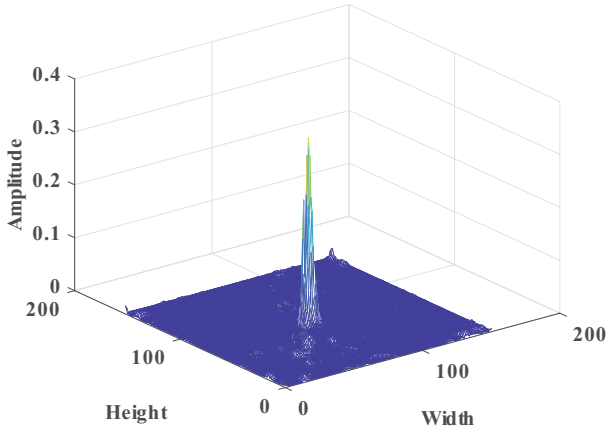

Figure 4. Sparse representation $\mathcal{H}(I_f)$ of filtered image I_f with 3D scene.

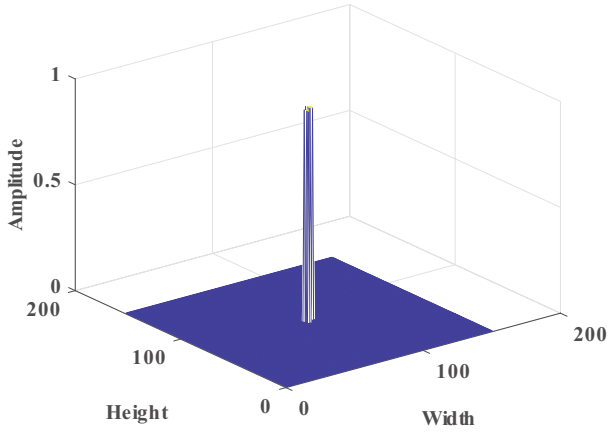

Figure 5. Segmented result I_c of $\mathcal{H}(I_f)$ with 3D scene.

Comparing the detection results using the SAR image, Fig. 6(a) and Fig. 6(b) show the detected-results by using CFAR detectors based on Gamma distribution [12] and k-wishart distribution [8], respectively. They tend to have many false alarms by using design parameters, target-window size 20×20, and the probability of false alarm $P_{fa} = 10^{-8}$. In fact, even if the detector is not CFAR for the true distribution of sea clutter, it will still only pick out bright pixel values. The results from these comparison indicate that the proposed detector performs much better for ship detection in SAR images.

Figure 6. Detected results by using CFAR detectors. (a) Gamma CFAR. (b) k-wishart CFAR.

4. CONCLUSIONS

This article proposes a novel detection method based on topological optimization method for ship detection in SAR images. Compared to CFAR detectors, the proposed detector fully takes advantage of the topological structure between ship targets and their surrounding clutter. It can achieve a good performance for ship detection, which has a great application value.

ACKNOWLEDGMENT

This work was supported in part by the National Natural Science Foundation of China (grants 61501152).

REFERENCES

1. Chen, S., X. Cui, X. Wang, and S. Xiao, "Speckle-free SAR image ship detection," *IEEE Trans. Image Process.*, Vol. 31, 5969–5983, 2021.
2. Pu, W., "Deep SAR imaging and motion compensation," *IEEE Trans. Image Process.*, Vol. 30, 2232–2247, 2021.
3. Pu, W., "Shuffle GAN with autoencoder: A deep learning approach to separate moving and stationary targets in SAR imagery," *IEEE Trans. Neural Networks and Learning Systems (Early Access)*, 1–15, 2021.
4. Lang, H., Y. Xi, and X. Zhang, "Ship detection in high-resolution SAR images by clustering spatially enhanced pixel descriptor," *IEEE Trans. Geosci. Remote Sens.*, Vol. 57, No. 8, 5407–5423, 2019.
5. Wang, X., Y. He, G. Li, and A. Plaza, "Adaptive superpixel segmentation of marine SAR images by aggregating Fisher vectors," *IEEE J. Sel. Topics Appl. Earth Observ.*, Vol. 14, 2058–2069, 2021.
6. Cui, X., Y. Su, and S. Chen, "A saliency detector for polarimetric SAR ship detection using similarity test," *IEEE J. Sel. Topics Appl. Earth Observ.*, Vol. 12, No. 9, 3423–3433, 2019.
7. Liu, T., Z. Yang, A. Marino, G. Gao, and J. Yang, "Robust CFAR detector based on truncated statistics for polarimetric synthetic aperture radar," *IEEE Trans. Geosci. Remote Sens.*, Vol. 58, No. 9, 6731–6747, 2020.
8. Liu, T., Z. Yang, J. Yang, and G. Gao, "CFAR ship detection methods using compact polarimetric SAR in a k-wishart distribution," *IEEE J. Sel. Topics Appl. Earth Observ.*, Vol. 12, No. 10, 3737–3745, 2019.
9. Zefreh, R., M. Taban, M. Naghsh, and S. Gazor, "Robust CFAR detector based on censored harmonic averaging in heterogeneous clutter," *IEEE Trans. Aeronaut. Navig. Electron.*, Vol. 57, No. 3, 1956–1963, 2021.
10. Xu, Z., C. Fan, S. Cheng, J. Wang, and X. Huang, "A distribution independent ship detector for PolSAR images," *IEEE J. Sel. Topics Appl. Earth Observ.*, Vol. 14, 3774–3786, 2021.
11. Larrabide, I., R. Feijóo, A. Novotny, and E. Taroco, "Topological derivative: A tool for image processing," *Comput. Struct.*, Vol. 86, No. 13, 1386–1403, 2008.
12. Gao, G., *Characterization of SAR Clutter and Its Applications to Land and Ocean Observations*, Springer, Singapore, 2019.